

# Strength and Nature of Host-Guest Interactions in Metal-Organic Frameworks from a Quantum-Chemical Perspective

Michelle Ernst<sup>\*[a, b]</sup> and Ganna Gryn'ova<sup>\*[a, b]</sup>

Metal-organic frameworks (MOFs) offer a convenient means for capturing, transporting, and releasing small molecules. Their rational design requires an in-depth understanding of the underlying non-covalent host-guest interactions, and the ability to easily and rapidly pre-screen candidate architectures *in silico*. In this work, we devised a recipe for computing the strength and analysing the nature of the host-guest interactions in MOFs. By assessing a range of density functional theory methods across periodic and finite supramolecular cluster scale

we find that appropriately constructed clusters readily reproduce the key interactions occurring in periodic models at a fraction of the computational cost. Host-guest interaction energies can be reliably computed with dispersion-corrected density functional theory methods; however, decoding their precise nature demands insights from energy decomposition schemes and quantum-chemical tools for bonding analysis such as the quantum theory of atoms in molecules, the non-covalent interactions index or the density overlap regions indicator.

## Introduction


Increasingly complex molecular structures have been developed to satisfy the ever-growing demand for highly efficient, multi-functional, and environmentally conscious materials. Among these, metal-organic frameworks (MOFs)<sup>[1,2]</sup> are attracting growing attention due to their highly tuneable composition, topologies, and physico-chemical properties. MOFs are porous crystalline hybrid inorganic-organic compounds that consist of regularly connected nodes and linkers, have high internal surface areas and low densities, and, most importantly for practical purposes, are able to absorb small guest molecules. The associated physisorption and chemisorption *via* host-guest interactions depends on the nature of the guest molecule, pore size and volume, surface area, solvent, etc. Numerous applications of MOFs hosting small molecules include gas storage and separation,<sup>[3,4]</sup> drug delivery,<sup>[5]</sup> (photo-)catalysis,<sup>[6,7]</sup> and biological imaging.<sup>[8–10]</sup>


Synthesis and characterisation of existing systems, as well as design and pre-screening of new and improved candidates require coordinated efforts from experiment and simulation. The myriad permutations of nodes and linkers into MOFs with distinct topologies, able to encapsulate molecular guests at varying loadings, require theory to rationally guide practice. Among the most commonly employed techniques to model the host-guest interactions in MOFs are grand-canonical Monte-Carlo (GCMC) and molecular dynamics (MD) simulations. The former are particularly well-suited for weakly interacting systems, such as gases in storage and catalysis applications,<sup>[11–14]</sup> but are also widely used to model the loading capacity of drug-delivering MOFs;<sup>[15–17]</sup> the latter are often employed to simulate diffusion of guests inside the pores.<sup>[16,18]</sup> These studies demonstrate not only the utility of GCMC and MD simulations to capture the structural features of MOFs and guests, but also the necessity to include quantum-chemical effects at the *ab initio* or density functional theory (DFT) level in order to explicitly examine the host-guest interactions.

However, modelling the intake of small molecules within MOFs using DFT and post-Hartree-Fock (post-HF) methods faces several challenges. First, MOFs are periodic systems that typically feature large and 'computationally expensive' unit cells with several metal atoms. Second, reliable experimental structures of the host-guest complexes that can serve as a starting point in subsequent geometry relaxation are rarely available. In such cases, a guess for the starting geometry can be generated using, for example, electrostatic complementarity.<sup>[19]</sup> Third, MOFs alone and, in particular, their complexes with small molecules are often disordered and rather dynamic. Consequently, most examples applying DFT and post-HF methods to MOFs focus on the uptake of very small compounds (e.g., gases and volatiles).<sup>[20–29]</sup> Periodic DFT studies on MOFs with larger guest molecules are somewhat less common.<sup>[19,30,31]</sup>

[a] Dr. M. Ernst, Dr. G. Gryn'ova  
Computational Carbon Chemistry Group  
Heidelberg Institute for Theoretical Studies (HITS gGmbH)  
69118 Heidelberg, Germany  
E-mail: michelle.ernst@h-its.org  
ganna.grynova@h-its.org

[b] Dr. M. Ernst, Dr. G. Gryn'ova  
Interdisciplinary Center for Scientific Computing  
Heidelberg University  
69120 Heidelberg, Germany

 Supporting information for this article is available on the WWW under <https://doi.org/10.1002/cphc.202200098>

 © 2022 The Authors. ChemPhysChem published by Wiley-VCH GmbH. This is an open access article under the terms of the Creative Commons Attribution Non-Commercial NoDerivs License, which permits use and distribution in any medium, provided the original work is properly cited, the use is non-commercial and no modifications or adaptations are made.

As an alternative to periodic approaches, the so-called 'cluster' computations focus on a finite-size model of the host-guest complex containing the interaction regions between the molecule and the MOF. Such a drastic decrease in the system size and conformational space opens the door to more accurate computations of complex geometries and interaction energies.<sup>[32–34]</sup> Moreover, it provides access to a broad range of sophisticated *in silico* techniques for quantifying, conceptualising, and visualising non-covalent interactions,<sup>[35]</sup> which, nonetheless, remain underutilised in MOF studies.<sup>[36]</sup> These quantum-chemical tools employ schemes for partitioning the multi-dimensional wavefunction and the total electron density into localised regions, as well as for decomposing the total interaction energy into physically meaningful components. Nowadays, these approaches are commonplace in studies on chemical stability and reactivity,<sup>[37–42]</sup> catalysis,<sup>[43–45]</sup> biomolecular interactions,<sup>[46,47]</sup> molecular crystals,<sup>[48–50]</sup> and organic electronics.<sup>[51–53]</sup> The purpose of this work is twofold: on the one hand, we demonstrate that these approaches can be applied to MOFs and provide meaningful insight into the host-guest interactions. On the other hand, we show that these conceptually different methods contribute to an all-encompassing comprehension of specific host-guest interactions.

Due to the aforementioned scarcity of accurate host-guest complex geometries, a profound theoretical understanding of the microscopic building blocks and their interactions is crucial for the rational design of new MOFs with desired adsorption properties. In this study, we probe the applicability and validity of diverse quantum-chemical tools for analysing and visualising the strength and physical nature of the non-covalent interactions in the MOF host-guest complexes across periodic and finite-size scales.

## Methodology

### Studied Systems

A MOF composed of nodes with calcium and oxygen atoms and adipate linkers was selected due to the availability of experimentally determined structures of its host-guest complexes.<sup>[54]</sup> In contrast to most MOF host-guest complexes, the guests are not disordered and were accurately determined. Two host-guest complexes of this MOF were considered: system 1 (CCDC refcode: PARHAS), containing 4,4'-bipyridine, and system 2 (CCDC refcode: PARHEW), containing 1,2-bis(4-pyridyl)ethane. Both systems crystallise in the monoclinic P21/c space group, but 2 has a slightly larger volume of 1934.94 Å<sup>3</sup> compared to 1752.46 Å<sup>3</sup> for 1. This is a consequence of the sizes of the guest molecules used as templates during synthesis. The framework is connected by adipate linkers in the *a* and *b* directions and by calcium and oxygen atoms in the *c* direction. The templating guest molecules reside in channels along the *c* direction. Each guest forms two distinct (not symmetry-related) hydrogen bonds with the host framework, in which the pyridinic nitrogen of the guest molecule is the hydrogen acceptor and the water molecule coordinated to the calcium of the framework is the hydrogen donor (Figure 1).

### Computational Methods

Constrained optimisation of the water molecules involved in the hydrogen bonds was performed to address the inaccurate assignment of the hydrogen atom positions in standard X-ray diffraction experiments (see SI for further discussion). These

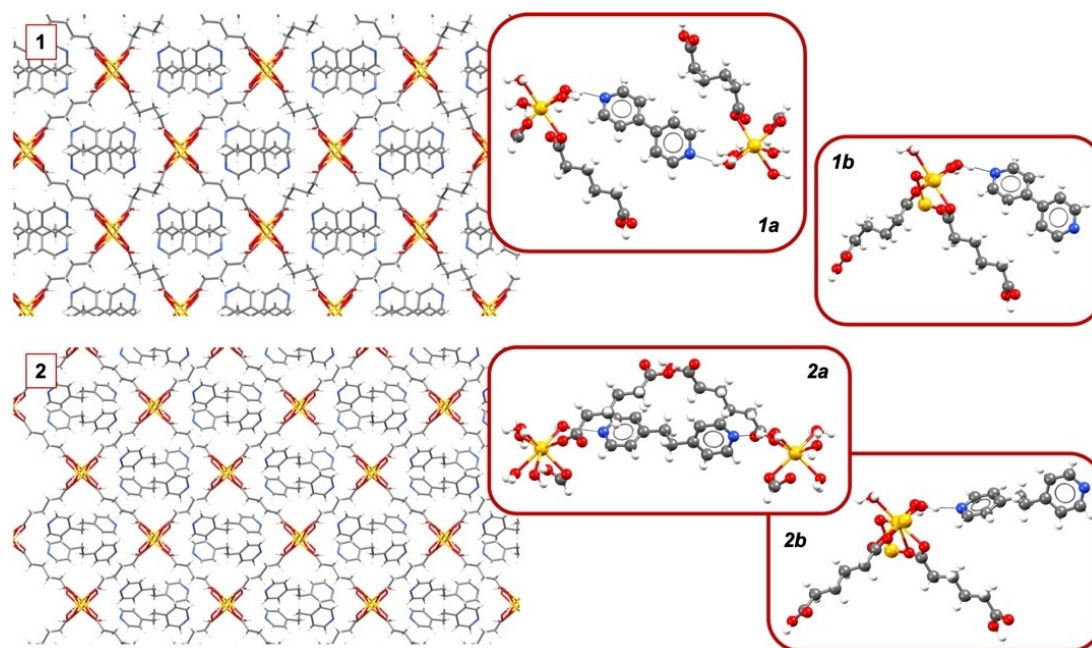


**Figure 1.** Crystal packing of systems 1 (4,4'-bipyridine guest) and 2 (1,2-bis(4-pyridyl)ethane guest), view in *c* direction. Inlet: the chosen cluster models for each complex. Hydrogen, carbon, nitrogen, oxygen, and calcium atoms are represented in white, grey, blue, red, and yellow colour, respectively.

geometry optimisations were performed at the B3LYP-D3<sup>[55]</sup>/pob-TZVP\_rev2<sup>[56]</sup> level of theory in a periodic setting with the shrinking factor set to 6 using Crystal17.<sup>[57]</sup> Interaction energies for the studied host-guest complexes in the so-obtained geometries were computed using periodic DFT with several functionals, namely B3LYP-D3, PBE0-D3, PBE-D3, LC- $\omega$ PBE-D3, M06-D3, and M06-2X-D3:

$$\Delta E = E_{hg} - [E_h + E_g] \quad (1)$$

where  $E_{hg}$  is the energy of the relaxed host-guest complex, and  $E_h$  and  $E_g$  are energies of the isolated host and guest molecules in their crystal geometries, respectively. Finally, the topology of the electron density in periodic computations was analysed in the framework of Bader's Quantum Theory of Atoms in Molecules (QTAIM)<sup>[58]</sup> using TOPOND<sup>[59]</sup> as implemented in Crystal17.<sup>[57]</sup>

Finite models of the host-guest complexes, denoted here as 'cluster' models, were constructed from experimental geometries of **1** and **2** with the partially optimised positions of the coordinated water molecules. For both systems, cluster models containing one guest molecule, hydrogen-bonded to MOF nodes, and the adjacent parts of the framework were defined. Clusters of two sizes, **a** and **b**, were considered where the smaller ones contain only the part of the framework forming the shortest interaction with the guest; and the larger ones contain the two shortest interactions and the corresponding framework parts (Figure 1). Terminal carboxylate groups of the adipates and unsaturated oxygen atoms of the metal node were hydrogenated for electric neutrality. Only the positions of these added hydrogen atoms were optimised, while the rest of the cluster was kept in the geometry from the periodic computations. Host-guest interaction energies (Eq. 2) in these clusters were computed using the same density functionals as in periodic computations in conjunction with a cc-pVTZ basis set and corrected for basis set superposition error (BSSE) using counterpoise correction:<sup>[60]</sup>

$$\Delta E = E_{hg} - [E_h + E_g] + E^{BSSE} \quad (2)$$

where  $E_{hg}$  is the electronic energy of the supramolecular cluster,  $E_h$  and  $E_g$  are electronic energies of the truncated host and guest molecule in their cluster geometries, and  $E^{BSSE}$  is the counterpoise correction. These computations were performed using Gaussian16.<sup>[61]</sup>

Features of the electron density in the studied cluster models were analysed by means of QTAIM<sup>[58]</sup> (at the B3LYP/cc-pVTZ level of theory using AIMAll<sup>[62]</sup>), the non-covalent interactions (NCI<sup>[63]</sup>) index (at the B3LYP/cc-pVTZ level of theory using NCIPLOT<sup>[64]</sup>), and the density overlap regions indicator (DORI,<sup>[65]</sup> at the B3LYP-D3/TZVP level of theory using ADF<sup>[66]</sup>). Furthermore, the total interaction energies in these complexes were analysed using two energy decomposition schemes: the energy decomposition analysis of Bickelhaupt and Baerends (BB-EDA,<sup>[67]</sup> at the B3LYP-D3/TZVP level using ADF<sup>[66]</sup>) and the symmetry-adapted perturbation theory (SAPT,<sup>[68]</sup> at the SAPT0/cc-pVTZ level using Psi4<sup>[69]</sup>).

## Results

### Periodic Model

#### Interaction Energy

Interaction energies, computed as per Eq. 1 at a periodic DFT level with several functionals including the D3 dispersion correction<sup>[55]</sup> are given in Figure 2 and Table S1 of the SI. MOF complex **2** is predicted to have stronger host-guest interactions relative to **1** with all considered methods; the gap between systems **1** and **2** is largest with LC- $\omega$ PBE-D3.

#### Electron Density Features

The topology of the electron density in the studied MOF complexes was analysed using QTAIM.<sup>[58]</sup> Since the primary host-guest interactions in systems **1** and **2** are through hydrogen bonds, the properties of their bond critical points (BCPs) were examined (Table 1). Trends in these properties are in line with the hydrogen bond lengths: shorter contacts in system **2** are associated with higher density  $\rho_{BCP}$  and Laplacian  $\nabla^2\rho_{BCP}$ , as well as more negative energy density  $H_{BCP}$ , relative to **1**.

### Cluster Model

#### Interaction Energy

Interaction energies in the supramolecular clusters (Eq. 2), obtained using several density functionals, are given in Figure 2 and Table S1 of the SI. While there is no substantial variation between the results at different levels of theory, the relative

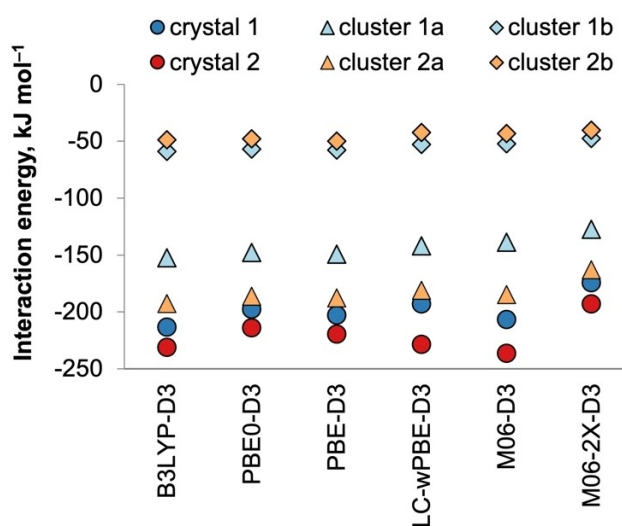


**Figure 2.** Host-guest interaction energies in periodic (Eq. 1; shown are interaction energies per guest molecule, *i. e.*  $\Delta E/4$ , as there are four guest molecules per unit cell) and cluster (Eq. 2) models of the studied systems, computed using a range of density functionals

**Table 1.** QTAIM analysis of the hydrogen bonds in the studied host-guest complexes and in a reference  $\text{NH}_3\cdots\text{H}_2\text{O}$  cluster.

System	Bond length [Å]	$\rho_{\text{BCP}}$ [a.u.]	$\nabla^2\rho_{\text{BCP}}$ [a.u.]	$H_{\text{BCP}}$ [a.u.]
Periodic model <sup>[d]</sup>				
1	1.883	0.035	0.090	$-3.35 \times 10^{-03}$
	1.904	0.033	0.086	$-2.87 \times 10^{-03}$
2	1.806	0.042	0.097	$-6.73 \times 10^{-03}$
	1.830	0.040	0.094	$-5.80 \times 10^{-03}$
Cluster model a <sup>[d]</sup>				
1	1.883	0.036	0.068	$-5.90 \times 10^{-03}$
	1.904	0.034	0.067	$-5.11 \times 10^{-03}$
2	1.806	0.044	0.064	$-1.04 \times 10^{-02}$
	1.830	0.041	0.064	$-9.14 \times 10^{-03}$
Cluster model b				
1	1.883	0.035	0.071	$-5.58 \times 10^{-03}$
2	1.806	0.043	0.072	$-9.59 \times 10^{-03}$
$\text{NH}_3\cdots\text{H}_2\text{O}$ cluster				
$\text{NH}_3\cdots\text{H}_2\text{O}$	1.700	0.048	0.088	$-1.15 \times 10^{-02}$
$\text{NH}_3\cdots\text{H}_2\text{O}$ (equilibrium)	1.954	0.031	0.069	$-3.00 \times 10^{-03}$
$\text{NH}_3\cdots\text{H}_2\text{O}$	2.200	0.018	0.049	$8.54 \times 10^{-04}$

[a]  $\rho_{\text{BCP}}$  is the electron density at the BCP. [b]  $\nabla^2\rho_{\text{BCP}}$  is the Laplacian at the BCP. [c]  $H_{\text{BCP}}$  is the energy density at the BCP. [d] Two lines for each of the studied complexes in the periodic model and clusters a correspond to the two hydrogen bonds, formed by each guest molecule with the framework.

interaction energies in the studied MOF-guest complexes are strongly influenced by the choice of the finite (cluster) model. The trend in  $\Delta E$  for the cluster model **a** closely resembles that from the periodic computations. Qualitatively, complex **2** is more stabilised than complex **1**; quantitatively,  $\Delta E$  values for cluster model **a** are 30–70  $\text{kJ mol}^{-1}$  above the interaction energies per guest molecule, computed for the periodic model. This is an unavoidable consequence of truncating an entire crystal with a multitude of interactions within it to a finite cluster. Cluster model **b** instead features much weaker (by as much as *ca.* 150  $\text{kJ mol}^{-1}$ ) interaction energies, with system **1** being more stabilised than system **2**.

To gain further insights into the nature of the host-guest interactions, decomposition analyses of the total interaction energies were performed. On one hand, within the energy decomposition framework of Bickelhaupt and Baerends (BB-EDA),<sup>[67]</sup> the interaction energy consists of:

- the *electrostatic interaction* between the fragments with initial (frozen) charge density distributions;
- the *exchange repulsion* arising from Pauli's principle and corresponding to the destabilisation due to antisymmetrisation of the wavefunction;
- the *orbital interaction energy* comprising the charge transfer among fragments and the polarisation within fragments resulting from orbital mixing and orbital relaxation; and
- the additional *dispersion* term, e.g., the D3 correction.

On the other hand, weak (compared to covalent bonds) intermolecular interactions can be treated as perturbations to the wavefunctions of the individual molecules. This approach is embodied by the symmetry-adapted perturbation theory (SAPT),<sup>[68]</sup> which provides access to accurate non-covalent interaction energies and their physically meaningful components:

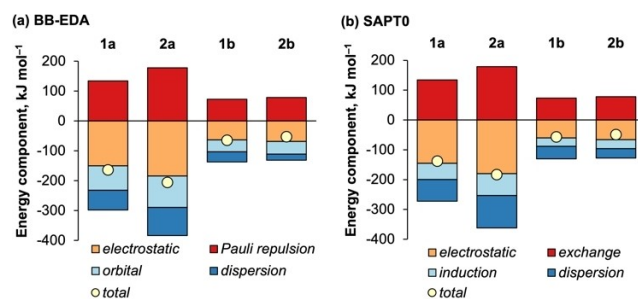
- the *electrostatic* energy arising from the electrostatic interaction of the two monomer electron densities;
- the *induction* energy reflecting the response of one electron density to polarisation by the other electron density;
- the *dispersion* energy due to mutual polarisation of the two fragments by instantaneous fluctuations of their densities; and
- the *exchange* energy due to Pauli's exclusion principle.

These two EDAs employ conceptually distinct approaches to quantifying the components of the total energy and thus allow for a comparative analysis of the studied systems. According to our results (Figure 3), the two schemes yield qualitatively similar pictures: the host-guest interaction in both **1** and **2** is primarily driven by electrostatics although orbital (induction) and dispersion interactions are also significant – a typical signature of hydrogen bonds.<sup>[70]</sup> All energy components are notably smaller in cluster model **b** than in **a**. Total interaction energies, computed with BB-EDA and SAPT0, are concordant with each other and with the DFT results.

### Electron Density Features

The chosen QTAIM<sup>[58]</sup> descriptors of the hydrogen bonds at their bond critical points in the supramolecular clusters are given in Table 1, and follow the same trends as in the periodic simulations. The electron densities at the BCPs in supramolecular clusters are almost identical to those obtained for the periodic model, while the Laplacian and energy density are only slightly lower.

To put these results in perspective, we compared them with a prototypical hydrogen-bonded dimer,  $\text{NH}_3\cdots\text{H}_2\text{O}$ , at three interaction distances (Table 1, see also Figure S4 in the SI). As a consequence of their crystal packing, systems **1** and **2** feature shorter hydrogen bonds than that of the fully relaxed  $\text{NH}_3\cdots\text{H}_2\text{O}$ . In general, the shorter the hydrogen bond, the higher the


**Figure 3.** Energy decomposition analyses in cluster models **a** and **b** of MOF-guest complexes **1** and **2**.



electron density and the Laplacian.<sup>[71]</sup> The energy density at the BCP is close to zero in all studied systems, as is typical for hydrogen bonds. These values are slightly negative, indicative of a somewhat predominated covalent character according to the criteria of Cremer and Kraka.<sup>[72]</sup>

The deformation density plots (Figure 4a) reveal two regions with an accumulation of electron density in the studied supramolecular clusters: (i) the aforementioned hydrogen bonds between the MOF's water molecule and the guest's pyridinic nitrogen, and (ii) a less obvious interaction between the guest's C<sub>Ar</sub>-H group and the oxygen atom of the adipate linker. The non-covalent interactions index<sup>[63]</sup> exploits the features of the electron density, its second derivative and reduced density gradient to analyse and visualise NCIs. A detailed discussion of the NCI analyses of the studied cluster models is available in the SI, while computed isosurfaces of the reduced density gradient are shown in Figure 4b. Finally, supramolecular clusters were analysed by means of the density overlap regions indicator (DORI),<sup>[65]</sup> which, unlike the NCI index, captures covalent and non-covalent interactions simultaneously (Figure 4c). Both the NCI index and DORI identify the same interaction patterns – pronounced hydrogen bonding between the framework's water molecule and the guest's pyridinic nitrogen, as well as additional interactions between the host's adipate backbone and the guest's C<sub>Ar</sub>-H groups – all in clear agreement with the results of the deformation density analysis.

Both tools also indicate, albeit on a qualitative level, that for cluster model **a**, the interactions are more numerous and pronounced in complex **2** than in **1**, while the opposite occurs in cluster model **b**.

## Discussion

The choice of a finite model for a periodic system can have important effects on its qualitative description. We demonstrate this by comparing the computed interaction energies for cluster models **a** and **b** to those for the periodic model, as well as to the indirect experimental evidence. Specifically, thermogravimetric analysis in the original study of the two calcium-adipate MOFs, GWMOF-7 (here complex **1**) and GWMOF-8 (here complex **2**),<sup>[54]</sup> suggests that complex **2** features somewhat stronger interactions between MOF and guest than complex **1**. This is reflected in the interaction energies, computed for the periodic model and cluster model **a**, but not cluster model **b**. The latter therefore does not provide adequate representation of the host-guest interactions. In light of the scarcity of accurate structural data for other MOF-guest complexes, our results stress the need for sufficiently large models in order to have any interpretative or predictive value in this domain.

Provided an appropriate finite model is chosen, it can be analysed with a plethora of quantum-chemical tools to obtain

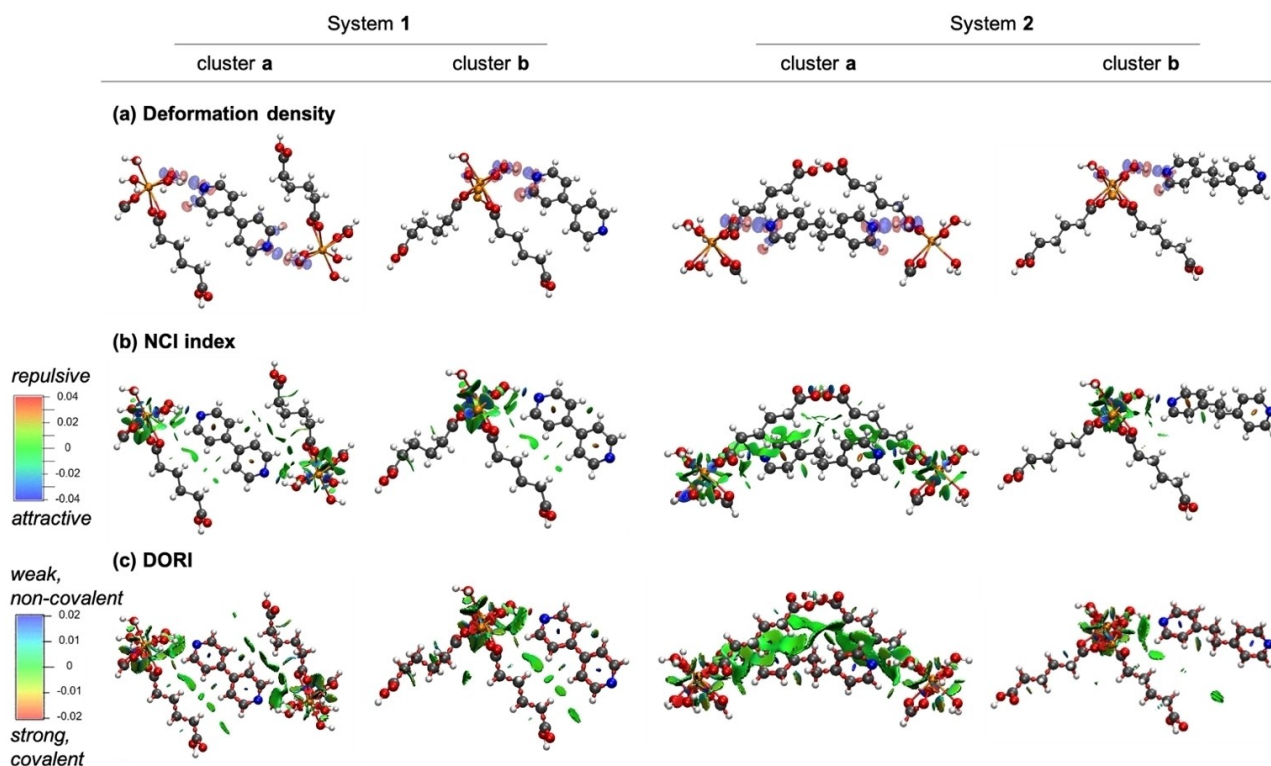


**Figure 4.** (a) Deformation density: full cluster density minus the sum of the fragment densities (blue and red represent positive and negative values, respectively; the surface isovalue is 0.002 a.u.). (b) NCI index surfaces corresponding to  $s = 0.5$  a.u. and the colour scale  $-0.04$  a.u. (blue)  $< \rho < 0.04$  a.u. (red). (c) DORI surfaces at 0.98 isovalue, colour-coded by  $\text{sign}(\lambda_2)\rho(r)$  in the range from  $-0.02$  a.u. (red) to  $0.02$  a.u. (blue). Note the opposite colour schemes for NCI and DORI surfaces, chosen in accordance with the literature standards. Hydrogen, carbon, nitrogen, oxygen, and calcium atoms are represented in white, grey, blue, red, and yellow colour, respectively.

valuable insights into the nature of the interactions between the host framework and its molecular guest. First, direct comparison of the QTAIM results between the periodic and cluster models reveals their strong quantitative agreement, further validating the ability of a suitable finite model to describe the non-covalent interactions in the real system. In the case of the species studied herein, the primary host-guest interaction, *i.e.*, the hydrogen bonds between the guest's pyridinic nitrogen and the MOF's water molecule, are shorter and consequently stronger in system 2 compared to 1 (Table 1). The NCI index and DORI results for the supramolecular clusters (Figure 4) confirm the predominant role of these hydrogen bonds in the interaction between MOF and guest. Thus, the 'obvious' hydrogen bonds are readily captured by all the tools employed in both the periodic and finite models. Furthermore, NCI and DORI indicate that other weakly stabilising interactions between the guest and the framework occur and are more abundant in system 2 than in system 1. These results highlight the need for both local, such as QTAIM, and global, *e.g.* NCI and DORI, bonding analyses to fully capture the relevant non-covalent interactions.

Finally, all energy components are larger in complex 2 than complex 1 with both the Bickelhaupt-Baerends and SAPT energy decomposition analyses (Figure 3) in agreement with the QTAIM, NCI, and DORI results. While both systems feature a significant stabilising electrostatic component corresponding to hydrogen bonding, the most pronounced difference between them arises from dispersion. This further emphasises the crucial role of secondary host-guest interactions.

## Conclusions

We investigated the strength and nature of non-covalent interactions between small molecules and a metal-organic framework host with a range of computational chemistry tools using periodic and finite (cluster) models. On the basis of the results obtained here, the following methodological implications for future *in silico* modelling of these systems arise. First, the choice of a supramolecular cluster representing the MOF-molecule complex is crucial for computing qualitatively correct interaction energies and analysing the non-covalent interactions responsible for them. In this work, two types of cluster model led to contrasting results, with the larger model accurately reproducing the data from periodic computations. Importantly, DFT and wavefunction-theory computations are still practicable for the larger clusters studied herein. Second, all tested dispersion-corrected density functionals, including general gradient approximation (GGA), hybrid, meta-GGA, and long-range corrected methods, yield qualitatively similar results for interaction energies with both infinite and cluster models. These DFT results are also in agreement with the total interaction energies obtained using two energy decomposition schemes, the Bickelhaupt-Baerends EDA and the symmetry-adapted perturbation theory. Despite being conceptually different in their treatment of various energy components, these EDA schemes yield a very similar qualitative picture for the studied

MOF complexes in agreement with literature results on other systems.<sup>[73]</sup> Comparing their performance against the periodic energy decomposition analyses<sup>[74]</sup> could be an ultimate validation; however, such tools have not yet been adapted specifically to MOFs. Third, excellent agreement between the results of Bader's quantum theory of atoms in molecules for crystal and cluster models supports the transferability of the qualitative trends from finite to periodic systems, provided the former are chosen appropriately. However, the QTAIM analysis itself is only suitable for studying the specific, pre-selected interactions. A more generalised, albeit rather qualitative, picture of the non-covalent interactions in MOFs can be achieved with the help of the non-covalent interactions index and the density overlap regions indicator. The latter two approaches enable the detection and visualisation of various intermolecular interactions, as well as qualitative assignment of their nature, *e.g.*, attractive *vs.* repulsive, and strong *vs.* weak. DORI has an added benefit of capturing the inter- and intramolecular interactions simultaneously.

A deeper understanding of the underlying interactions in MOF-guest complexes, afforded by the quantum-chemical tools tested here, can enhance the rational design of MOFs toward target applications. In this work, we have demonstrated that tools such as QTAIM, NCI index, and DORI, commonplace in the domain of small molecule modelling, have immense utility when transferred to organic frameworks. Many such tools are currently practical only for cluster models; however, the latter, when constructed carefully, yield reliable energies and types of non-covalent interactions when compared to periodic results.

## Acknowledgements

The authors acknowledge support from the Klaus Tschira Foundation. M.E acknowledges support from the Swiss National Science Foundation (project number: P2BEP2\_195236). The authors thank the state of Baden-Württemberg through bwHPC (bwForCluster JUSTUS2) and the University of Bern (HPC cluster UBELIX, <http://www.id.unibe.ch/hpc>) for granting access to computational resources. The authors thank Dr John Lindner for proof-reading the manuscript. Open Access funding enabled and organized by Projekt DEAL.

## Conflict of Interest

The authors declare no conflict of interest.

## Data Availability Statement

The data that support the findings of this study are available in the supplementary material of this article.

**Keywords:** metal-organic frameworks · noncovalent interactions · host-guest complexes · adsorption · materials design

- [1] B. F. Hoskins, R. Robson, *J. Am. Chem. Soc.* **1990**, *112*, 1546–1554.
- [2] O. M. Yaghi, H. Li, *J. Am. Chem. Soc.* **1995**, *117*, 10401–10402.
- [3] B. Li, H.-M. Wen, W. Zhou, B. Chen, *J. Phys. Chem. Lett.* **2014**, *5*, 3468–3479.
- [4] H. Li, K. Wang, Y. Sun, C. T. Lollar, J. Li, H.-C. Zhou, *Mater. Today* **2018**, *21*, 108–121.
- [5] P. Horcajada, C. Serre, M. Vallet-Regí, M. Sebban, F. Taulelle, G. Férey, *Angew. Chem. Int. Ed.* **2006**, *45*, 5974–5978; *Angew. Chem.* **2006**, *118*, 6120–6124.
- [6] F. Llabres i Xamena, A. Abad, A. Corma, H. Garcia, *J. Catal.* **2007**, *250*, 294–298.
- [7] U. Ravon, M. E. Domine, C. Gaudillère, A. Desmartin-Chomel, D. Farrusseng, *New J. Chem.* **2008**, *32*, 937–940.
- [8] P. F. Muldoon, G. Collet, S. V. Eliseeva, T.-Y. Luo, S. Petoud, N. L. Rosi, *J. Am. Chem. Soc.* **2020**, *142*, 8776–8781.
- [9] A. Foucault-Collet, K. A. Gogick, K. A. White, S. Villette, A. Pallier, G. Collet, C. Kieda, T. Li, S. J. Geib, N. L. Rosi, S. Petoud, *Proc. Natl. Acad. Sci. USA* **2013**, *110*, 17199–17204.
- [10] S. Zhang, X. Pei, H. Gao, S. Chen, J. Wang, *Chin. Chem. Lett.* **2020**, *31*, 1060–1070.
- [11] R. B. Getman, Y.-S. Bae, C. E. Wilmer, R. Q. Snurr, *Chem. Rev.* **2012**, *112*, 703–723.
- [12] Y.-Z. Li, G.-D. Wang, H.-Y. Yang, L. Hou, Y.-Y. Wang, Z. Zhu, *Inorg. Chem. Front.* **2020**, *7*, 746–755.
- [13] D.-Y. Ma, Z. Li, J.-X. Xiao, R. Deng, P.-F. Lin, R.-Q. Chen, Y.-Q. Liang, H.-F. Guo, B. Liu, J.-Q. Liu, *Inorg. Chem.* **2015**, *54*, 6719–6726.
- [14] V. Bernales, M. A. Ortuño, D. G. Truhlar, C. J. Cramer, L. Gagliardi, *ACS Cent. Sci.* **2018**, *4*, 5–19.
- [15] M. C. Bernini, D. Fairen-Jimenez, M. Pasinetti, A. J. Ramirez-Pastor, R. Q. Snurr, *J. Mater. Chem. B* **2014**, *2*, 766–774.
- [16] R. Babarao, J. Jiang, *J. Phys. Chem. C* **2009**, *113*, 18287–18291.
- [17] M. Kotzabasaki, G. E. Froudakis, *Inorg. Chem. Front.* **2018**, *5*, 1255–1272.
- [18] T. Mueller, G. Ceder, *J. Phys. Chem. B* **2005**, *109*, 17974–17983.
- [19] M. Delle Piane, M. Corno, A. Pedone, R. Dovesi, P. Ugliengo, *J. Phys. Chem. C* **2014**, *118*, 26737–26749.
- [20] R. Scatena, Y. Guntern, P. Macchi, *J. Am. Chem. Soc.* **2019**, *141*, 9382–9390.
- [21] T. Watanabe, S. Keskin, S. Nair, D. S. Sholl, *Phys. Chem. Chem. Phys.* **2009**, *11*, 11389–11394.
- [22] L. Grajciar, O. Bludský, P. Nachtigall, *J. Phys. Chem. Lett.* **2010**, *1*, 3354–3359.
- [23] Y.-H. Kim, J. Kang, S.-H. Wei, *Phys. Rev. Lett.* **2010**, *105*, 236105.
- [24] K. Sillar, A. Hofmann, J. Sauer, *J. Am. Chem. Soc.* **2009**, *131*, 4143–4150.
- [25] K. Sillar, J. Sauer, *J. Am. Chem. Soc.* **2012**, *134*, 18354–18365.
- [26] M. Dixit, T. A. Maark, S. Pal, *Int. J. Hydrogen Energy* **2011**, *36*, 10816–10827.
- [27] R. Poloni, B. Smit, *J. Am. Chem. Soc.* **2012**, *134*, 6714–6719.
- [28] H. Kim, Y. Jung, *J. Phys. Chem. Lett.* **2014**, *5*, 440–446.
- [29] L. C. Gallington, I. S. Kim, W.-G. Liu, A. A. Yakovenko, A. E. Platero-Prats, Z. Li, T. C. Wang, J. T. Hupp, O. K. Farha, D. G. Truhlar, A. B. F. Martinson, K. W. Chapman, *J. Am. Chem. Soc.* **2016**, *138*, 13513–13516.
- [30] P. Horcajada, C. Serre, G. Maurin, N. A. Ramsahye, F. Balas, M. Vallet-Regí, M. Sebban, F. Taulelle, G. Férey, *J. Am. Chem. Soc.* **2008**, *130*, 6774–6780.
- [31] C. Vieira Soares, G. Maurin, A. A. Leitão, *J. Phys. Chem. C* **2019**, *123*, 19077–19086.
- [32] E. N. Koukaras, T. Montagnon, P. Trikalitis, D. Bikiaris, A. D. Zdetsis, G. E. Froudakis, *J. Phys. Chem. C* **2014**, *118*, 8885–8890.
- [33] M. Kotzabasaki, I. Galdadas, E. Tylanakis, E. Klontzas, Z. Cournia, G. E. Froudakis, *J. Mater. Chem. B* **2017**, *5*, 3277–3282.
- [34] Y. Yao, X. Song, J. Qiu, C. Hao, *J. Phys. Chem. A* **2014**, *118*, 6191–6196.
- [35] E. Pastorczak, C. Corminboeuf, *J. Chem. Phys.* **2017**, *146*, 120901.
- [36] J. L. Mancuso, A. M. Mroz, K. N. Le, C. H. Hendon, *Chem. Rev.* **2020**, *120*, 8641–8715.
- [37] M. Busch, R. B. Wang, A. Hellman, J. Rossmels, H. Grönbeck, *J. Phys. Chem. C* **2018**, *122*, 216–226.
- [38] I. Casademont-Reig, T. Woller, J. Contreras-García, M. Alonso, M. Torrent-Sucarrat, E. Matito, *Phys. Chem. Chem. Phys.* **2018**, *20*, 2787–2796.
- [39] L. J. Karas, A. T. Campbell, I. V. Alabugin, J. I. Wu, *Org. Lett.* **2020**, *22*, 7083–7087.
- [40] I. Fernández, G. Frenking, *Eur. J. Org. Chem.* **2019**, 478–485.
- [41] R. Lee, G. Gryn'ova, K. U. Ingold, M. L. Coote, *Phys. Chem. Chem. Phys.* **2016**, *18*, 23673–23679.
- [42] M. Fugel, M. V. Ponomarenko, M. F. Hesse, L. A. Malaspina, F. Kleemiss, K. Sugimoto, A. Genoni, G.-V. Röschenthaler, S. Grabowsky, *Dalton Trans.* **2019**, 48, 16330–16339.
- [43] B. W. Bakra, C. D. Sherrill, *Phys. Chem. Chem. Phys.* **2018**, *20*, 18241–18251.
- [44] R. M. H. Ugale, S. E. Wheeler, *Chem. Eur. J.* **2019**, *25*, 4452–4459.
- [45] P. Vermeeren, T. A. Hamlin, F. M. Bickelhaupt, I. Fernández, *Chem. Eur. J.* **2020**, *27*, 5180–5190.
- [46] M. J. S. Phipps, T. Fox, C. S. Tautermann, C.-K. Skylaris, *Chem. Soc. Rev.* **2015**, *44*, 3177–3211.
- [47] D. Arias-Olivares, E. K. Wieduwilt, J. Contreras-García, A. Genoni, *J. Chem. Theory Comput.* **2019**, *15*, 6456–6470.
- [48] B. Meyer, S. Barthel, A. Mace, L. Vannay, B. Guillot, B. Smit, C. Corminboeuf, *J. Phys. Chem. Lett.* **2019**, *10*, 1482–1488.
- [49] N. Casati, A. Kleppe, A. Jephcoat, P. Macchi, *Nat. Commun.* **2016**, *7*, 10901.
- [50] C. Foroutan-Nejad, M. Straka, I. Fernández, G. Frenking, *Angew. Chem. Int. Ed.* **2018**, *130*, 14127–14130.
- [51] P. R. Varadwaj, A. Varadwaj, H. M. Marques, K. Yamashita, *Sci. Rep.* **2019**, *9*, 50.
- [52] Z. Wen, J. I.-C. Wu, *Chem. Commun.* **2020**, *56*, 2008–2011.
- [53] G. Gryn'ova, C. Corminboeuf, *J. Phys. Chem. Lett.* **2016**, *7*, 5198–5204.
- [54] D. T. de Lill, D. J. Bozzuto, C. L. Cahill, *Dalton Trans.* **2005**, *12*, 2111–2115.
- [55] J. Moellmann, S. Grimme, *J. Phys. Chem. C* **2014**, *118*, 7615–7621.
- [56] D. Vilela Oliveira, M. F. Peintinger, J. Laun, T. Bredow, *J. Comb. Chem.* **2019**, *40*, 2364–2376.
- [57] a) R. Dovesi, A. Erba, R. Orlando, C. M. Zicovich-Wilson, B. Civalieri, L. Maschio, M. Rerat, S. Casassa, J. Baima, S. Salustro, B. Kirtman, Quantum-Mechanical Condensed Matter Simulations with CRYSTAL. *WIRES Comput. Mol. Sci.* **2018**, *8*, e1360; b) R. Dovesi, V. R. Saunders, C. Roetti, R. Orlando, C. M. Zicovich-Wilson, F. Pascale, B. Civalieri, K. Doll, N. M. Harrison, I. J. Bush, P. D'Arco, M. Llunell, M. Causà, Y. Noël, L. Maschio, A. Erba, M. Rerat, S. Casassa, CRYSTAL17, (2017) CRYSTAL17 User's Manual. University of Torino, Torino.
- [58] R. F. W. Bader, *Acc. Chem. Res.* **1985**, *18*, 9–15.
- [59] C. Gatti, V. R. Saunders, C. Roetti, *J. Chem. Phys.* **1994**, *101*, 10686.
- [60] S. Simon, M. Duran, J. J. Dannenberg, *J. Chem. Phys.* **1996**, *105*, 11024–31.
- [61] Gaussian 16 (Revision C.01), M. J. Frisch, G. W. Trucks, H. B. Schlegel, G. E. Scuseria, M. A. Robb, J. R. Cheeseman, G. Scalmani, V. Barone, G. A. Petersson, H. Nakatsuji, X. Li, M. Caricato, A. V. Marenich, J. Bloino, B. G. Janesko, R. Gomperts, B. Mennucci, H. P. Hratchian, J. V. Ortiz, A. F. Izmaylov, J. L. Sonnenberg, D. Williams-Young, F. Ding, F. Lipparini, F. Egidi, J. Goings, B. Peng, A. Petrone, T. Henderson, D. Ranasinghe, V. G. Zakrzewski, J. Gao, N. Rega, G. Zheng, W. Liang, M. Hada, M. Ehara, K. Toyota, R. Fukuda, J. Hasegawa, M. Ishida, T. Nakajima, Y. Honda, O. Kitao, H. Nakai, T. Vreven, K. Throssell, J. A. Montgomery, Jr., J. E. Peralta, F. Ogliaro, M. J. Bearpark, J. J. Heyd, E. N. Brothers, K. N. Kudin, V. N. Staroverov, T. A. Keith, R. Kobayashi, J. Normand, K. Raghavachari, A. P. Rendell, J. C. Burant, S. S. Iyengar, J. Tomasi, M. Cossi, J. M. Millam, M. Klene, C. Adamo, R. Cammi, J. W. Ochterski, R. L. Martin, K. Morokuma, O. Farkas, J. B. Foresman, and D. J. Fox, Gaussian, Inc., Wallingford CT, **2016**.
- [62] AIMAll (Version 19.10.12), T. A. Keith and T. K. Gristmill Software, Overland Park KS, USA, **2019** (aim.tkgristmill.com).
- [63] E. R. Johnson, S. Keinan, P. Mori-Sánchez, J. Contreras-García, A. J. Cohen, W. Yang, *J. Am. Chem. Soc.* **2010**, *132*, 6498–6506.
- [64] J. Contreras-García, E. R. Johnson, S. Keinan, R. Chaudret, J.-P. Piquemal, D. N. Beratan, W. Yang, *J. Chem. Theory Comput.* **2011**, *7*, 625–632.
- [65] P. de Silva, C. Corminboeuf, *J. Chem. Theory Comput.* **2014**, *10*, 3745–3756.
- [66] a) G. te Velde, F. M. Bickelhaupt, E. J. Baerends, C. Fonseca Guerra, S. J. A. van Gisbergen, J. G. Snijders, T. Ziegler, *J. Comput. Chem.* **2001**, *22*, 931–967; b) ADF 2019.304, SCM, Theoretical Chemistry, Vrije Universiteit, Amsterdam, The Netherlands, <http://www.scm.com>.
- [67] F. M. Bickelhaupt, E. J. Baerends, *Rev. Comput. Chem.* **2000**, *15*, 1–86.
- [68] B. Jeziorski, R. Moszynski, K. Szalewicz, *Chem. Rev.* **1994**, *94*, 1887–1930.
- [69] R. M. Parrish, L. A. Burns, D. G. A. Smith, A. C. Simmonett, A. E. DePrince III, E. G. Hohenstein, U. Bozkaya, A. Y. Sokolov, R. Di Remigio, R. M. Richard, J. F. Gonthier, A. M. James, H. R. McAlexander, A. Kumar,

- M. Saitow, X. Wang, B. P. Pritchard, P. Verma, H. F. Schaefer III, K. Patkowski, R. A. King, E. F. Valeev, F. A. Evangelista, J. M. Turney, T. D. Crawford, C. D. Sherrill, *J. Chem. Theory Comput.* **2017**, *13*, 3185–3197.
- [70] S. C. C. van der Lubbe, C. Fonseca-Guerra, *Chem. Asian J.* **2019**, *14*, 2760–2769.
- [71] E. Espinosa, I. Alkorta, J. Elguero, E. Molins, *J. Chem. Phys.* **2002**, *117*, 5529.
- [72] D. Cremer, E. Kraka, *Croat. Chem. Acta* **1984**, *57*, 1259–1281.
- [73] O. A. Stasyuk, R. Sedlak, C. Fonseca Guerra, P. Hobza, *J. Chem. Theory Comput.* **2018**, *14*, 3440–3450.
- [74] M. Raupach, R. Tonner, *J. Chem. Phys.* **2015**, *142*, 194105.

---

Manuscript received: February 9, 2022  
Accepted manuscript online: February 14, 2022  
Version of record online: February 24, 2022

---